2017 IEEE 56th Annual Conference on Decision and Control (CDC)
December 12-15, 2017, Melbourne, Australia

A Real-time Eco-Driving Strategy for Automated Electric Vehicles

Luis LEON OJEDA, Jihun HAN, Antonio SCIARRETTA, Giovanni DE NUNZIO, Laurent THIBAULT

***Abstract*— Over the past years, connected and automated vehicles (CAV) have become highly important in the transportation research field. Several prototypes are already introduced by established companies in cooperation with research centers. However, the crucial part of reducing their energy consumption by driving in an optimal way and facing external disturbances is sometimes overlooked. In this paper, we propose a safe- and eco-driving control system that enables the CAV to accelerate or to decelerate optimally while preventing both collision with preceding vehicle (i.e. disturbance) and violation of speed limitations. Optimal control problem (OCP) minimizing energy consumption for an electric vehicle while enforcing state constraints is formulated. Numerically, the problem is solved using a Model Predictive Control-like approach. The real-time implementation is possible thanks to the analytical solution of the state-constrained OCP. The proposed system is evaluated through a simulation for various driving scenarios, and it is shown that it can significantly reduce energy consumption compared to conventional driving while also avoiding the collision, without increasing arrival time.**

***Index Terms*— Real-time eco-driving, model predictive control, electric vehicles, connected and automated vehicles.**

I. Introduction

Eco-driving, or *hypermiling*, is defined as the use of energy-saving driving techniques to maximize the vehicle's energy efficiency. Eco-driving control has been very popular and studied widely over the past decade given its direct effects on decreasing environmental pollution. Existing works can be divided into two categories as follows: heuristic strategies and model-based strategies. The former are based on eco-driving rules such as: aggressiveness of the acceleration, stability of the cruising speed, anticipation and aggressiveness of the deceleration and braking, duration of idling, or optimal gear changing [1]. The latter use optimal control techniques to solve the following eco-driving control problem.

$$\begin{array}{rl} \textit{minimize} & \text{cost function,} \\ \textit{subject to} & \text{system dynamics,} \\ & \text{physical constraints,} \\ & \text{state constraints,} \end{array} \tag{1}$$

where the cost function indicates control objective (e.g. energy consumption), system dynamics represents vehicle dynamics, and includes additional dynamics (e.g. battery dynamics in case of hybrid electric vehicles). Physical constraints indicate the control constraints imposed by actuator limitation (e.g. electric motor). State constraints are defined by the vehicle safety such as maintaining the speed in its allowable range and keeping a minimal safety distance with the preceding vehicle.

Optimal solution has different forms depending on the type of vehicle as well as on the advanced driver-assistance system (ADAS) [2]. In general, the above formulated OCP can be solved in different ways: 1) Dynamic Programming (DP), 2) direct methods, and 3) indirect methods [3]. Both, DP and direct methods, require quantization of state and/or control variables to approximate the original OCP, thereby resulting in the trade-off between accuracy and computational demand. In [4] for instance, position constraint imposed by preceding vehicle is introduced and the DP is used to compute the constrained optimal solution that guarantees a minimum safety distance. Given its large computational burden, this solution cannot be implementable in real-time. On the other hand, indirect methods use the first-order optimality conditions, which is referred to as Pontryagin's Minimum Principle (PMP), to solve OCPs without quantization, and thus lead to low computational time. The PMP can, itself, be solved analytically or numerically (Boundary value problem, BVP).

Research on adaptive cruise control (ACC) that enables automatic driving has been highlighted in the field of optimization under constraint on state variables and control inputs. Nevertheless, a few study attempts to reduce energy consumption while minimizing original cost such as tracking the speed and maintaining the minimum safety distance. To make ecological ACC feasible in a real-time scenario, a fast numerical algorithm based on PMP (e.g. continuation and generalized minimum residual (C/GMRES) method [5]) is used to solve multi-objective nonlinear model predictive control (MPC) problem. These energy-efficient ACCs can achieve reduction of energy consumption by predicting the upcoming traffic states [6] or by predicting driving behavior of the preceding vehicle [7], [8], based on road and traffic signal information.

Energy-efficient ACC optimizes the speed within a limited range due to inherent property of speed tracking, whereas speed advisory system can consider full range of the speed by defining energy consumption as sole cost function. Many studies have proposed algorithm to generate optimal speed profile. Specially, in [9], [10], the authors introduce analytical unconstrained solution and show its effectiveness on reduction of energy consumption. Furthermore, [11] presents analytical speed-constrained solution taking account of model parameter evolving by gear shift and road grade and the near-optimal energy consumption while reducing computational time significantly, compared to DP solution. However, this approach does not include the vehicle safety constraint,

L. LEON OJEDA, J. HAN, A. SCIARRETTA, G. DE NUNZIO, L. THIBAULT, Department of Control Signal and Systems, IFPen, Rueil-Malmaison, France, {*luis-leon.ojeda, jihun.han, antonio.sciarretta, giovanni.de-nunzio, laurent.thibault*}*@ifpen.fr*

thereby occurring collision with the preceding vehicle. Using analytical solution as the speed advisory system is also applied for connected and automated vehicle system. In [12], [13], unconstrained solution is used to coordinate multiple CAVs at highway on-ramps and urban traffic intersections in order to pass at the right moments and optimally.

This paper defines sole cost function like the speed advisory system, but takes account of speed limitations and vehicle safety as state constraints, in order to apply the proposed algorithm for CAV. In this context, it is assumed that the host vehicle can measure or estimate the state of itself and the preceding vehicle (acceleration, speed, and position). The problem is formulated as an OCP and solved using the MPC-like approach. The solution obtained from the unconstrained OCP proposed in [9] is extended to state-constrained solution via PMP. Therefore, the main contributions of this paper are as follows. First, a constrained analytical solution is derived, considering speed and position limitations. Second, an analytical MPC is proposed for the real-time application. And third, the proposed MPC scheme is validated for different speed profiles of the preceding vehicle.

The reminder of the paper is organized as follows, Sec. II presents a short background of the state-constrained OCP. Sec. III outlines the system equations and the MPC formulation. In Sec. IV, the applied algorithm is explained in detail. The application in different testing scenarios is described in Sec. V. Finally in Sec. VI, the main contributions of the paper are summarized and possible future research directions are outlined.

II. Background on State-Constrained Optimal Control Problem

A generic state-constrained OCP can be written as follows:

$$\begin{array}{ll} \textit{minimize} & J = \int_0^{t_f} l(u, \mathbf{x}, t) \\ \textit{subject to} & \dot{\mathbf{x}}(t) = f(u, \mathbf{x}, t), \\ & \mathbf{x} \in \mathbf{X}, u \in U \end{array} \tag{2}$$

where J and l are the cost functional and the cost function, respectively. $\mathbf{x}$ and u represent state vector and control input, respectively; X and U are admissible state and control ranges.

A. General State Inequality Constraints

The above OCP might have *mixed state inequality constraints* and/or *pure state inequality constraints*. The pure state inequality constraints do not explicitly depend on a control variable, and thus they are difficult to handle in PMP. If the number of pure state inequality constraints is r, the ith constraint is described in the following form:

$$h_i(\mathbf{x}, t) < 0, \qquad i = 1, 2, \cdots, r. \tag{3}$$

The *order* (or relative order) of the pure state inequality constraints can be defined by consecutively time-differentiating them until the control variable explicitly appears [14]. Therefore, the pth order of the ith constraint is expressed as follows,

$$[h_i^{(p)}]_u \neq 0, \quad [h_i^{(k)}]_u = 0, \qquad k = 1, 2, \cdots, p-1, \tag{4}$$

where the *pth order constraint*, $[h_i^{(p)}]_u$, is directly dependent on the control variable. Note that $[h_i^{(p)}]_u$ represents the *mixed state inequality constraints*.

For the ith constraint, an interval $[\tau_1, \tau_2]$ with $\tau_1 < \tau_2$ is called a *boundary interval* if $h_i(x, t) = 0$ for $t \in [\tau_1, \tau_2]$. The time, τ_1 (or τ_2), is called an *entry time* (or *exit time*) at which the boundary interval starts (or ends), and if the state trajectory just touches the boundary at a specific time (i.e. $h_i(x, \tau) = 0$), this time, τ, is called a *contact time*, where the entry, exit, and contact times are called *junction times*.

B. Analytical Approach: Indirect Adjoining Method

From the cost function and state equations, Hamiltonian can be defined using *Lagrange multiplier* (i.e. *co-state* variable) as follows:

$$H(u, \mathbf{x}, \boldsymbol{\lambda}, t) = l(u, \mathbf{x}, t) + \boldsymbol{\lambda}^T f(u, \mathbf{x}, t), \tag{5}$$

There are two main ways to adjoin the pure state inequality constraints in the Hamiltonian: *direct* and *indirect adjoining* method [15]. The direct adjoining method directly adjoins the state constraint in the Hamiltonian, whereas the indirect adjoining method adjoins the pth order state constraint (the mixed constraint) in the Hamiltonian in indirect way. Although the resulting formulations are different in the two cases, two necessary conditions are essentially equivalent if the OCP is sufficiently smooth. In this paper, the indirect adjoining method is used in order to derive a closed-form solution.

For simplicity, it is assumed there is only one pure state constraint with order $p \geq 2$ in the OCP. Then, the Lagrangian is formed by adjoining the pth order state constraints with a new Lagrange multiplier, μ, as follows:

$$L(u, \mathbf{x}, \boldsymbol{\lambda}, \eta, t) = H(u, \mathbf{x}, \boldsymbol{\lambda}, t) + \mu h^{(p)}(u, \mathbf{x}, \boldsymbol{\lambda}), \tag{6}$$

where control region is $\Omega(\mathbf{x}, t) = \{h^{(p)} \leq 0 \text{ if } h = 0\}$.

Furthermore, since the implicit control of state constraints might not keep the state trajectory on the boundary interval alone, the following *tangency condition* of the pth order constraint at the junction times must be satisfied:

$$\Psi(\mathbf{x}, t) \doteq \begin{bmatrix} h^{(0)}(\mathbf{x}, t) \\ h^{(2)}(\mathbf{x}, t) \\ \vdots \\ h^{(p-1)}(\mathbf{x}, t) \end{bmatrix} = 0. \tag{7}$$

The above tangency condition can be treated as interior-point constraints with unspecified entry time in $[0, t_f]$. Thus, using p-component vector of constant Lagrange multipliers $(\pi^0, \cdots, \pi^{p-1})$, the interior-point constraints can be adjoined in the cost functional. Namely, the pure state constraints are replaced by the interior-point constraints (7) and the mixed constraints ($h^{(p)}(u, \mathbf{x}, t) \leq 0$) along the boundary

interval. From this formulation, the necessary conditions for optimality are described as follows:

$$\begin{aligned} u^*(t) &= \arg\min_{u\in\Omega(x^*,t)} H(u^*,\mathbf{x}^*,\boldsymbol{\lambda}^*,t), \\ \dot{\mathbf{x}}^*(t) &= L^*_{\boldsymbol{\lambda}}(u^*,\mathbf{x}^*,\boldsymbol{\lambda}^*,\mu^*,t), \\ \dot{\boldsymbol{\lambda}}^*(t) &= L^*_{\mathbf{x}}(u^*,\mathbf{x}^*,\boldsymbol{\lambda}^*,\mu^*,t), \end{aligned} \tag{8}$$

where $\mu^*(t)h^{(p)}(u^*,\mathbf{x}^*,t)=0, \quad \mu^*(t)\geq 0.$

At every entry time, the co-state and the Hamiltonian might have discontinuities of the form

$$\begin{aligned} \boldsymbol{\lambda}^*(\tau^-)^T &= \boldsymbol{\lambda}^*(\tau^+)^T + \textstyle\sum_{j=0}^{p-1}\pi_j h^{(j)}_{\mathbf{x}^*}(\mathbf{x}^*,\tau), \\ H(\tau^-) &= H(\tau^+) - \textstyle\sum_{j=0}^{p-1}\pi_j h^{(j)}_t(\mathbf{x}^*,\tau). \end{aligned} \tag{9}$$

III. Eco-driving control Problem Formulation

In this section, an electric vehicle model is introduced, and an MPC problem is formulated for eco-driving studies.

A. Transmission and vehicle longitudinal model

If no losses in the transmission and no slip at wheels are considered, the transmission model is written as:

$$\begin{aligned} F_t &= (T_m \eta_t^{\text{sign}(T_m)} R_t)/r, \\ \omega_m &= (vR_t)/r, \end{aligned} \tag{10}$$

where F_t is the traction force, T_m the motor torque, R_t is transmission ratio, η_t is transmission efficiency, v is the longitudinal speed, r is the wheel radius, and ω_m is rotational motor speed.

From Newton's third law, the vehicle's longitudinal dynamic model is expressed using resistance forces (such as air drag resistance, F_a, rolling resistance, F_r, and gravity, F_g) and the mechanical brake force, F_b, as follows:

$$\begin{aligned} \dot{s} &= v, \\ m\dot{v} &= F_t - F_a - F_r - F_g - F_b, \\ &= \tfrac{R_t}{r} T_m \eta_t^{\text{sign}(T_m)} - \tfrac{1}{2}\rho_a A_f c_d v^2 - mgc_r - \\ &\quad - mg\sin(\alpha(s)) - F_b, \end{aligned} \tag{11}$$

where m is the vehicle's mass, ρ_a is the external air density, A_f is the vehicle frontal area, c_d is the aerodynamic drag coefficient, c_r is the rolling resistance coefficient, α is the road slope as a function of the position s, and g is the gravity.

B. Energy consumption model

Electric motor power is modeled as steady state map as a function of the motor torque and the rotational speed. In this paper, an approximated DC motor model for the electric motor power is used to derive analytical formula of optimal control input from PMP, as follows:

$$\begin{aligned} P_m &= V_a i_a, \\ &= \omega_m T_m + \tfrac{R_a}{k^2} T_m^2, \\ &= b_1 uv + b_2 u^2, \end{aligned} \tag{12}$$

where $b_1 := \frac{vR_t}{r}$, and $b_2 := \frac{R_a}{k^2}$. V_a, i_a, and R_a are armature voltage, current, and resistance, respectively. k is the speed constant. The control variable is defined as the motor torque, $u =: T_m$. Note that $V_a = i_a R_a + k\omega_m$ and $i_a = \frac{T_m}{k}$.

C. MPC problem formulation

In this paper, two types of state constraint are considered; position constraint with minimum safe distance (δ_s), $s \leq s_p - \delta_s$, and speed constraint, $v \leq v_{max}$. They play a significant role in avoiding the rear-end collision with the preceding vehicle and in not exceeding maximum speed, respectively. Note that s_p indicates the position imposed by the preceding vehicle, and v_{max} indicates maximum speed. Using longitudinal vehicle dynamics and constraints on control and state, eco-driving problem minimizing energy consumption is formulated as an MPC problem. In the MPC framework, the motor torque is computed as the solution of a constrained OCP over a finite time horizon (*prediction horizon*, t_p), and this procedure is repeated using newly updated current state variables in a feedback way at every time step.

$$\begin{aligned} \text{minimize} \quad & J = \textstyle\int_{t_0}^{t_0+t_p} b_1 uv + b_2 u^2 \mathrm{d}t, \\ \text{subject to} \quad & \dot{s}(t) = v, \\ & \dot{v}(t) = c_1 u \eta_t^{\text{sign}(u)} - c_2 v^2 - c_0 - W, \\ & s(t) \leq s_p(t) - \delta_s, \quad v(t) \leq v_{max}, \\ & u_{min} \leq u(t) \leq u_{max}, \\ & s(t_0) = s_0, \quad s(t_0+t_p) = s_f, \\ & v(t_0) = v_0, \quad x(t_0+t_p) = v_f, \end{aligned} \tag{13}$$

where t_0 is current time. $c_1 := \frac{R_t}{rm}$, $c_2 := \frac{1}{2m}\rho_a A_f c_d$, $c_0 := gc_r + g\sin(\alpha(s))$, $W := \frac{F_b}{m}$.

The nonlinear MPC problem requires a nonlinear optimization solver (e.g. direct collocation method) to compute the optimal control input profile. It is generally accepted that when the prediction horizon length increases, the MPC could improve the performance up to global optimum, but could not be implemented in real-time because of a large computational burden. In this paper, through required assumptions, the MPC problem comes to be analytically solved. Using the analytical solution leads to low computational time regardless of the prediction horizon length. With this benefit, the prediction horizon can be defined as from current time to the desired final time. The detailed procedure to derive the analytical solution is addressed in next section.

IV. Analytical MPC

For simplicity, $[t_0, t_0+t_p]$ is rewritten as $[0, t_p]$. To derive analytical solution using the indirect adjoining method, further assumptions are required, that is: 1) no transmission loss ($\eta_t = 1$), 2) no friction braking torque ($W = 0$), 3) no control input constraints ($u_{max} = -u_{min} \to \infty$), 4) no aerodynamic friction ($c_2 = 0$), 5) flat road ($\alpha(s) = 0$), and 6) constant acceleration of the preceding vehicle ($a_p(t) = a_{p.0}$, $t \in [0, t_p]$).

A. Unconstrained Solution

In absence of the state constraints, there is only one phase in which the resulting optimal control is a linear function of time, as follows:

$$u^*(t) = k_1 t + k_2, \tag{14}$$

where $k_1 = (b_1 c_0 + c_1 \lambda_{s.0})/(2b_2)$, $k_2 = -(b_1 v_0 + c_1 \lambda_{v.0})/(2b_2)$.

With two boundary conditions (such as $v^*(t_p) = v_f$, $s^*(t_p) = s_f$), the unconstrained optimal state trajectory is expressed as a polynomial function of time [10].

B. Speed Only Constrained Solution

Speed constraint (maximum speed bound) is defined as $h_v^{(0)} = v - v_{max} \leq 0$ and is of the first order, since $h_v^{(1)} = c_1 u - c_0$. Using the necessary conditions, the jump conditions are described, as follows:

$$\begin{aligned} \lambda_s^*(\tau^-) &= \lambda_s^*(\tau^+), \\ \lambda_v^*(\tau^-) &= \lambda_v^*(\tau^+) + \pi_0, \\ H(\tau^-) &= H(\tau^+). \end{aligned} \tag{15}$$

From above jump conditions and continuous control input, the jump parameter of speed co-state variables, π_0, is zero, thereby resulting in the continuity of both co-state variables without any jumps. The speed constraint can be active only on the boundary interval, which leads to three phases of an optimal control, as described below.

$$u^*(t) = \begin{cases} k_1 t + k_2 & [0, \tau_1^-] \\ u_{c.v} & [\tau_1^+, \tau_2^-] \\ k_1(t - \tau_2) + u_{c.v} & [\tau_2^+, t_p] \end{cases}, \tag{16}$$

where a boundary control input, $u_{c.v}$, is defined by $h_v^{(1)} = c_1 u_{c.v} - c_0 = 0$, i.e. the host vehicle is driving at maximum speed.

Since there are two interior-point conditions (i.e. $u^*(\tau_1) = u_{c.v}$, $v^*(\tau_1) = v_{max}$) and two boundary conditions, four unknown parameters (i.e. $\lambda_{v.0}$, $\lambda_{s.0}$, τ_1, τ_2) can be determined by solving four algebraic equations.

C. Position Only Constrained Solution

With assumption of the constant acceleration of the preceding vehicle, the speed and position are expressed in the following form, $v_p(t) = a_{p.0} t + v_{p.0}$, $s_p(t) = \frac{1}{2} a_{p.0} t^2 + v_{p.0} t + s_{p.0}$, where $v_{p.0}$ and $s_{p.0}$ denote the speed and position of the preceding vehicle at the current time, respectively. In order to prevent rear-end collision between two consecutive vehicles, the position constraint (maximum position bound) is defined as $h_s^{(0)} = s(t) - s_p(t) + \delta_s \leq 0$ and is of the second order, since $h_s^{(1)} = v - (a_{p.0} t + v_{p.0})$ and $h_s^{(2)} = c_1 u - c_0 - a_{p.0}$. The jump conditions are described as follows:

$$\begin{aligned} \lambda_s^*(\tau^-) &= \lambda_s^*(\tau^+) + \pi_0, \\ \lambda_v^*(\tau^-) &= \lambda_v^*(\tau^+) + \pi_1, \\ H(\tau^-) &= H(\tau^+) + \{\pi_0(a_{p.0}\tau + v_{p.0}) + \pi_1 a_{p.0}\}. \end{aligned} \tag{17}$$

The position co-state, $\lambda_s^*(t)$, is discontinuous at the entry time because of non-zero jump parameter, π_0. On the other hand, another jump parameter, π_1, should be zero, i.e., the speed co-state, $\lambda_v^*(t)$, is continuous. The second-order state variable inequality constraint generally becomes active either on the boundary interval or at the contact point depending on whether its mixed constraint ($h_s^{(2)} \leq 0$) is active or not if $h_s = 0$ [14].

Optimal control of the boundary interval case (i.e. $h_s^{(2)} = 0$) is expressed in the similar form as the speed only constrained case, as follows:

$$u^*(t) = \begin{cases} k_1 t + k_2 & [0, \tau_1^-] \\ u_{c.s} & [\tau_1^+, \tau_2^-] \\ k_3(t - \tau_2) + u_{c.s} & [\tau_2^+, t_p] \end{cases}, \tag{18}$$

where $k_3 = k_1 + (c_1 \pi_0)/(2b_2)$ and a boundary control, $u_{c.s}$, is defined by $h_s^{(2)} = c_1 u_{c.s} - c_0 - a_{p.0} = 0$, i.e., the host vehicle is driving exactly the same as the preceding vehicle with minimum safe distance.

On the other hand, the contact point case has two phases of optimal control due to inactive mixed constraint, as follows:

$$u^*(t) = \begin{cases} k_1 t + k_2 & [0, \tau_1^-] \\ k_3(t - \tau_1) + u^*(\tau_1^-) & [\tau_1^+, t_f] \end{cases}, \tag{19}$$

where optimal state touches the boundary at τ_1.

Five or four unknown parameters (i.e. $\lambda_{v.0}$, $\lambda_{s.0}$, π_0, τ_1 with/without τ_2) can be determined by using three or two interior-point conditions (i.e. $v^*(\tau_1) = v_p(\tau_1)$, $s^*(\tau_1) = s_p(\tau_1)$ with/without $u^*(\tau_1) = u_{c.s}$) and two boundary conditions.

As shown in the example of Fig. 1 with $\delta_s = 0$, two possible schemes separately occur corresponding to the initial speed of the host vehicle. As the initial speed increases, the position constraint is firstly active at the contact point, then it starts to be active on the boundary interval and also increases the length of the boundary interval by decreasing the entry time, in order to enforce the mixed constraint. Fig. 2. shows the solutions for two different initial speed. It is observed that for a finite range of the initial speed value, the following vehicle behaves exactly in the same way as the preceding vehicle on the boundary arc.

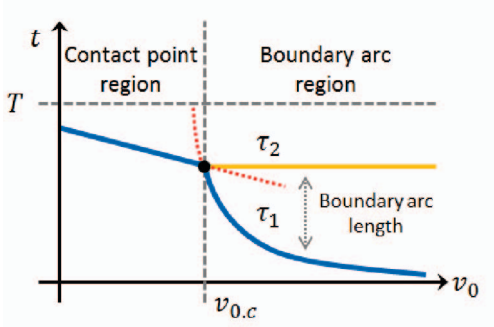

Fig. 1: Classification of region for position only constrained solution: τ_1 and τ_2 indicate entry and exit time, respectively.

D. Both Speed and Position Constrained Solution

When both speed and position constraints become active, the solution has several sequences depending on the location of the junction times. For example, the position constraint is

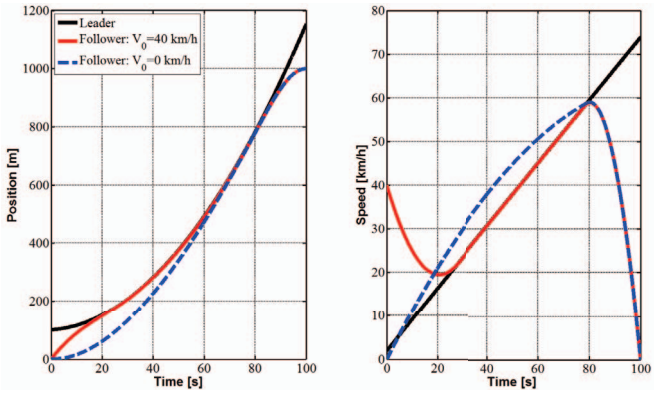

Fig. 2: Results of position only constrained solution with two different values of initial speed. $V_0 = 40km/h$ for boundary interval case, $V_0 = 0km/h$ for contact point case.

firstly active at the contact point and then the speed constraint is active on the boundary interval. The corresponding optimal control is expressed as follows:

$$u^*(t) = \begin{cases} k_1 t + k_2 & [0, \tau_1^-] \\ k_3(t-\tau_1) + u^*(\tau_1^-) & [\tau_1^+, \tau_2^-] \\ u_{c.v} & [\tau_2^+, \tau_3^-] \\ k_3(t-\tau_3) + u_{c.v} & [\tau_3^+, t_f] \end{cases}, \tag{20}$$

In the same way of the above example, based on the interior-point and boundary conditions, the unknown parameters can be determined. Possible combinations of the junction times are simultaneously calculated and then the proper one satisfying the prescribed correct order in $[0, t_f]$ is selected for future driving situations.

V. Simulation Results

A. Test design

In the following, simulation environments are presented. The goals of this subsection are as follows: to validate the assumption of simplified models, and to assess the proposed method in a driving situation. The vehicle parameters are $m = 1432$ kg, $r = 0.2820$ m, $R_t = 9.59$, $\eta_t = 0.98$. The MPC updating period is set to 0.1 s and maximum speed is set to 50 km/h.

We evaluate the performance of the proposed approach by using the percentage error as energy metric, *loss of energy optimality (L_{OPT})*:

$$L_{OPT} = \frac{\|E_{MPC} - E_{OPT}\|}{E_{OPT}} \times 100\% \tag{21}$$

where E_{MPC} and E_{OPT} indicate respectively the final energy consumption using the proposed approach and the optimal solution using an interior penalty method (BVP) [16]. Note that a nonlinear BVP solver (e.g. collocation method, bvp5c or bvp4c function in MATLAB [17]) is used, and several iterations are performed to obtain E_{OPT} as a penalty parameter decreases. The energy consumption is normalized by the distance traveled.

B. Simple driving scenario

Test parameters. ***Host vehicle***: initial conditions ($s_0 = 0$ m, $v_0 = 0$ km/h) and terminal conditions ($s_f = 1000$ m, $v_f = 0$ km/h, $t_f = 80$ s). ***Preceding vehicle***: $s_{p.0} = 100$ m, $v_{p.0} = 36$ km/h, $a_{p.0} = 0.04$ m/s^2.

We consider a simple driving scenario that activates both speed and position constraint, where the preceding vehicle is driving with a constant acceleration. As shown in Fig. 3, the MPC generates nearly same speed and position trajectories as the non-linear BVP optimal solution. Although the MPC cannot generate several modes (such as coasting and mechanical braking mode in [2]), it results in near-optimal energy performance ($L_{OPT} = 3.62\%$). This result indicates that the MPC framework can compensate for the loss of information caused by the required assumption of the simplified model. As benchmark, the non-linear BVP solver guarantees its optimality, but its solution cannot be directly implemented because of the large computational time.

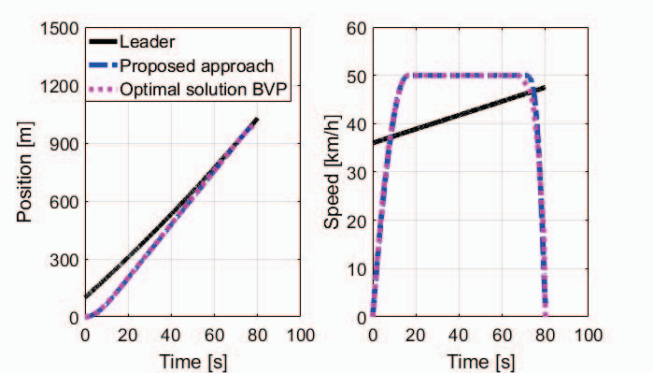

Fig. 3: Results of a simple driving scenario: trajectory of a) position and b) speed.

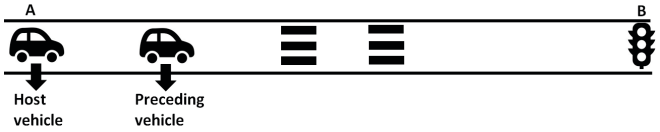

Fig. 4: Aimsun network scenario from point A to point B.

C. Aimsun scenario

Test parameters. ***Host vehicle***: initial conditions ($s_0 = 0$ m, $v_0 = 0$ km/h) and terminal conditions ($s_f = 904$ m, $v_f = 0$ km/h, $t_f = 84$ s). ***Preceding vehicle***: $s_{p.0} = 25$ m.

In this section, Aimsun Simulator is used to evaluate the performance of the proposed method. The Gipps' model provided from Aimsun is also used as a comparison, which represents non-eco-driving vehicle. The scenario is based on a follower-leader situation, in which both vehicles travel from point A to point B passing through two consecutive pedestrian crossings as shown in Fig. 4. The CAV is forced to arrive at destination at the time same as the leader. The test aims to evaluate how the proposed approach adapts to driving disturbances of the preceding vehicle. To that end,

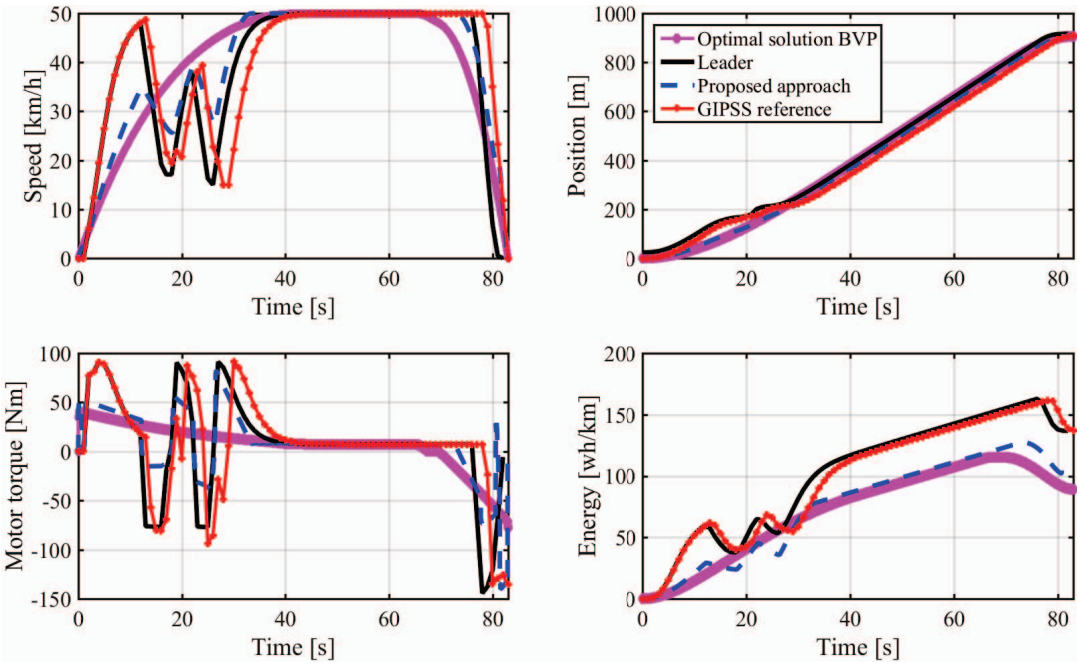

Fig. 5: Results for an Aimsun scenario: a) Speed profiles, b) Trajectories, c) Torque profiles, d) Energy.

the preceding vehicle will pass through a "slowdown zone" imposed by the pedestrian crossings.

Results are shown in Fig. 5. It is observed how the proposed method performs well while facing a disturbance. Fig. 5-a shows that the safe- and eco-driving vehicle quickly adapts its speed according to the changes measured from the leader. Thus, it arrives at the crossings at a lower speed with respect to the non-eco-driving vehicle, with less sharp acceleration and deceleration phases. Between $t = 40$ s and $t = 70$ s all drivers behave similarly, whereas when the red light is approaching, the safe- and eco-driving vehicle anticipates the stop of the preceding vehicle in contrast with the non-eco-driving vehicle. Furthermore, it is observed that the constraint imposed by the leader's position is respected (Fig. 5-b), while resulting in less aggressive torque profile (Fig. 5-c). Note that, although no constraints on the control input were imposed in order to obtain an analytical solution, the motor torque stays within a feasible range. Lastly, Fig. 5-d shows that in terms of energy consumption performance, the safe- and eco-driving vehicle outperforms the non-eco-driving vehicle by 31.15 % due to the smoothness of its speed.

In order to describe various scenarios for a given route, the leader's microscopic parameters are changed, as shown in Tab. I. Resulting several scenarios are used to compute the energy metric (L_{OPT}) of the proposed method and Gipps' model. Note that the boundary conditions of the proposed method are extracted from the results of the Gipps' model for fair comparison. As shown in Fig. 6, the proposed method achieves sub-optimal performance of energy consumption (8 % in average), while the Gipps' model results in significant losses of energy optimality (42 % in average). The Gipps' model's performance is sensitive to the leader's driving behavior due to its inherent property of following the leader without the prediction (35 % as minimum and 52 % as maximum). On the other hand, the proposed method shows the robust performance towards driving uncertainty of the leader (7.5 % as minimum and 9.5 % as maximum).

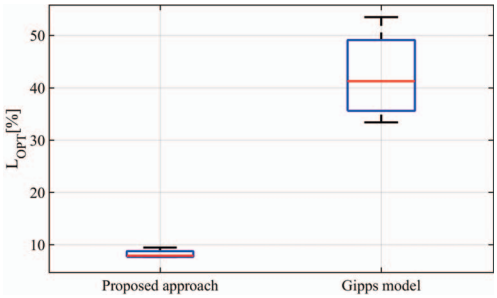

Fig. 6: Box plot showing the loss of energy optimality for the proposed approach and Gipps' model from Aimsun.

D. Real driving scenario

Test parameters. ***Host vehicle***: initial conditions ($s_0 = 0$ m, $v_0 = 0$ km/h) and terminal conditions ($s_f = 1073$ m, $v_f = 0$ km/h, $t_f = 142$ s). ***Preceding vehicle***: $s_{p.0} = 75$ m.

Finally, a real driving scenario is considered. The preceding vehicle is assumed to drive at a real-world speed profile. The real profile is obtained from a trip from a real-world database. In Fig. 7-a between 70 and 130 s, the proposed algorithm generates similar speed profile with the preceding vehicle due to consideration of the preceding vehicle's braking. On the other hand, the optimal BVP perfectly knows future driving behavior of the preceding vehicle, and thus it does not generates braking regardless of the preceding vehicle's vehicle's braking during a trip. As

TABLE I: Variation of Aimsun microscopic parameters

Maximum acceleration $[m/s^2]$	4.5	4.0	4.0	3.5	3.85	2.0	2.75	5.0
Maximum braking $[m/s^2]$	6.0	5.5	4.0	2.5	5.25	5.5	3.0	3.0

for the non-eco-driving vehicle, a phase of sharp acceleration is found until the moment it follows the profile of the leader. Fig. 7-b shows interesting energy results. As expected, BVP provides the best solution, followed by the proposed approach, then by the non-eco-driving vehicle and finally by the energy of the leader. The loss of optimality (L_{OPT}) was computed for both, the proposed and Gipps' method, and the results are $L_{OPT,MPC} = 8.60\%$ and $L_{OPT,Gipps} = 20.43\%$. These results are consistent with those found using Aimsun, showing that the proposed approach is also adapted to real-world scenarios.

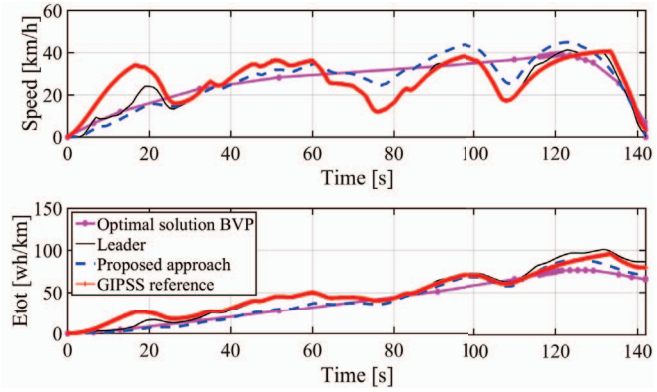

Fig. 7: Results for a real workd scenario: a) Speed profiles, b) Energy.

VI. Conclusions and future work

A novel safe- and eco-driving control system, based on analytical solution, has been proposed in this paper. The vehicle safety considered as the state constraints can be combined with original eco-driving control problem that defines the energy consumption as sole cost function. This eco-driving control problem is formulated as a model predictive control (MPC) problem. Through the MPC framework, optimal control input is computed as the solution of constrained optimal control problem over the prediction horizon, with predicting the preceding vehicle's trajectory under the assumption of constant acceleration. The primary novelty is the use of an analytical solution in the core of the MPC, which makes this algorithm suitable for a real-time use. The proposed method is validated for various driving profiles for the preceding vehicle. The simulation results show that the proposed method yields robust and near-optimal energy consumption while avoiding the collision with the preceding vehicle as well as maintaining the speed within its admissible range, compared to non-eco-driving vehicle. Future work will consider the computation of an analytical solution by considering road grade, road geometry, and aggressiveness of other drivers, as well as the use of a more complicated model to predict the surrounding vehicles' state.

References

[1] L. Chao-Yang and S. Yu-Ci, *Intelligent Eco-driving Guidance for Autonomous Driver System*. Changhua County, (Taiwan): Green Vehicle Development Division Automotive Research and Testing Center.

[2] A. Sciarretta, G. De Nunzio, and L. Leon Ojeda, "Optimal ecodriving control: Energy-efficient driving of road vehicles as an optimal control problem," *Control Systems, IEEE*, vol. 35, no. 5, pp. 71–90, Oct 2015.

[3] A. V. Rao, "Trajectory optimization: A survey," *Optimization and Optimal Control in Automotive Systems*, pp. 3–21, 2014. [Online]. Available: http://link.springer.com/chapter/10.1007%2F978-3-319-05371-4_1

[4] F. Mensing, E. Bideaux, R. Trigui, and H. Tattegrain, "Trajectory optimization of electric vehicles for eco-driving applications," *Transportation Research Part D: Transport and Environment*, vol. 18, 1 2013.

[5] T. Ohtsuka, "A continuation/gmres method for fast computation of nonlinear receding horizon control," *Automatica*, vol. 40, pp. 563–574, 2004. [Online]. Available: http://www.sciencedirect.com/science/article/pii/S0005109803003637

[6] K. Yu, J. Yang, and D. Yamaguchi, "Model predictive control for hybrid vehicle ecological driving using traffic signal and road slope information," *Control Theory and Technology*, vol. 13, pp. 17–28, 2015.

[7] M. A. S. Kamal, M. Mukai, J. Murata, and T. Kawabe, "Model predictive control of vehicles on urban roads for improved fuel economyl," *IEEE Transactions on Control Systems Technology*, vol. 21, pp. 831–841, 2013. [Online]. Available: http://ieeexplore.ieee.org/stamp/stamp.jsp?tp=&arnumber=6214590&isnumber=6497562

[8] M. A. S. Kamal and T. Kawabe, "Eco-driving using real-time optimization," in *ECC 2015 - 14th European Control Conference*, Linz, Austria, July 2015.

[9] N. Petit and A. Sciarretta, "Optimal drive of electric vehicles using an inversion-based trajectory generation approach," in *18th IFAC World Congress*, Milano, Italy, Aug. 2011, pp. 14 519–14 526. [Online]. Available: https://hal-mines-paristech.archives-ouvertes.fr/hal-00646523

[10] W. Dib, A. Chasse, P. Moulin, A. Sciarretta, and G. Corde, "Optimal energy management for an electric vehicle in eco-driving applications," *Control Engineering Practice*, vol. 29, pp. 299 – 307, 2014. [Online]. Available: http://www.sciencedirect.com/science/article/pii/S0967066114000355

[11] U. Ozatay, Engin andOzguner and D. Filev, "Velocity profile optimization of on road vehicles: Pontryagin's maximum principle based approach," *Control Engineering Practice*, vol. 51, 9 2016.

[12] J. Rios-Torres and A. A. Malikopoulos, "Automated and cooperative vehicle merging at highway on-ramps," *IEEE Transactions on Intelligent Transportation Systems*, vol. PP, pp. 1–10, 2016. [Online]. Available: http://ieeexplore.ieee.org/stamp/stamp.jsp?tp=&arnumber=7534837&isnumber=4358928

[13] Y. J. Zhang, A. A. Malikopoulos, and C. G. Cassandras, "Optimal control and coordination of connected and automated vehicles at urban traffic intersections," in *2016 American Control Conference (ACC)*, Boston, MA, USA, July 2016, pp. 6227–6232.

[14] A. E. Bryson and Y.-C. Ho, *Applied optimal control: optimization, estimation, and control*. Washington, DC: CRC Press, 1975.

[15] R. F. Hartl, S. P. Sethi, and R. G. Vickson, "A survey of the maximum principles for optimal control problems with state constraints," *SIAM Review*, vol. 37, pp. 181–218, 1995. [Online]. Available: http://epubs.siam.org/doi/abs/10.1137/1037043

[16] P. Malisanil, F. Chaplais, and N. Petit, "An interior penalty method for optimal control problems with state and input constraints of nonlinear systems," *Optimal Control Applications and Methods*, vol. 37, pp. 3–33, 2016. [Online]. Available: http://onlinelibrary.wiley.com/doi/10.1002/oca.2134/abstract

[17] L. F. Shampine, J. Kierzenka, and R. M. W, "Solving boundary value problems for ordinary differential equations in matlab with bvp4c," 2000. [Online]. Available: http://www.mathworks.com/bvp_tutorial